17th World Conference on Earthquake Engineering, 17WCEE
Sendai, Japan - September 13th to 18th 2020

IMPROVED PANEL ZONE MODEL FOR SEISMIC DESIGN OF STEEL MOMENT RESISTING FRAMES

A. Skiadopoulos[(1)], A. Elkady[(2)], D.G. Lignos[(3)]

[(1)] *Doctoral Assistant, Swiss Federal Institute of Technology, Lausanne (EPFL), Switzerland, andronikos.skiadopoulos@epfl.ch*
[(2)] *Lecturer, University of Southampton, Southampton, United Kingdom, a.elkady@soton.ac.uk*
[(3)] *Associate Professor, Swiss Federal Institute of Technology, Lausanne (EPFL), Switzerland, dimitrios.lignos@epfl.ch*

Abstract

In capacity-designed steel moment resisting frames (MRFs), the column-web panel zones are designed to experience limited inelasticity. One of the main obstacles in letting the panel zone attain large inelastic distortion angles is the associated increase in the beam flange-to-column face weld fracture potential. Subassembly experiments indicate that properly detailed beam-to-column connections utilizing weak panel zones may possess a satisfactory seismic performance. However, a steppingstone in embracing a balanced design philosophy in steel MRFs is to have a robust panel zone model to accurately predict the panel zone joint shear resistance.

Available panel zone models are typically idealized with multi-linear models. These include; (a) an elastic branch up to uniform column web yielding; (b) an inelastic branch accounting for the contributions of the column flanges and continuity plates; and (c) a third branch to acknowledge the steel material's strain hardening, assuming that above a certain shear distortion the column flange contribution is negligible. With regard to the elastic branch, past studies demonstrated that the shear strain distribution is non-uniform at the onset of yielding, often leading to panel zone shear resistance overestimation. The second branch is defined based on calibrations with limited experimental data of scaled specimens (i.e., the column flange thicknesses are less than 25mm). This typically leads to a panel zone shear resistance overestimation by up to 40%.

This paper proposes an improved mechanics-based panel zone model that could be potentially used for the seismic design of steel MRFs. This model is based on rigorous continuum finite element (CFE) simulations validated with available experimental data. To investigate the current panel zone model discrepancies, the CFE models employ varying panel zone aspect ratios and column flange thicknesses. We propose an updated elastic stiffness that captures bending as well as shear deformations within the panel zone. We also propose expressions to predict the panel zone shear strength at three levels of shear distortions. These expressions account for the realistic stress distributions within the web panel and column flanges. Comparisons between the proposed model and available experimental data are presented. The proposed panel zone model demonstrates superior performance in predicting a panel zone's behavior compared to prior formulations.

Keywords: steel moment resisting frames; panel zone shear resistance; beam-to-column connections; panel zone

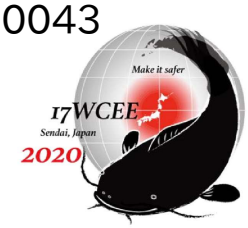

1. Introduction

Beam-to-column connections in steel moment-resisting frame (MRF) systems are designed such that the panel zone is not the primary dissipative element during an earthquake. Excessive kinking in the panel zone [1]–[4] may occur otherwise. Prior studies have highlighted the stable hysteretic response of beam-to-column connections when inelasticity is allowed in the panel zone [5]–[10]. To potentially exploit this beneficial dissipative mechanism in seismic design, a new panel zone model is needed to reliably predict the expected panel zone shear strength evolution while the shear distortion angle increases.

Referring to Fig. 1a, available panel zone models assume an elastic stiffness, K_e [see Eq. (1)] up to the onset of uniformly distributed yielding in the column web [11]. The corresponding panel zone shear strength at yield, V_y, is computed according to Eq. (2). After uniform web yielding, it is assumed that the column flanges and continuity plates (if present) contribute to the panel zone shear strength up to a shear distortion angle of $4\gamma_y$ (γ_y is the panel zone's yield shear distortion-angle). Accordingly, the plastic shear strength, V_p, is computed based on Eq. (3). Finally, beyond $4\gamma_y$, a third branch with a constant positive slope (stiffness) of $0.03K_e$ is assumed (see Fig. 1a). This model is known in the literature as the Krawinkler model [11].

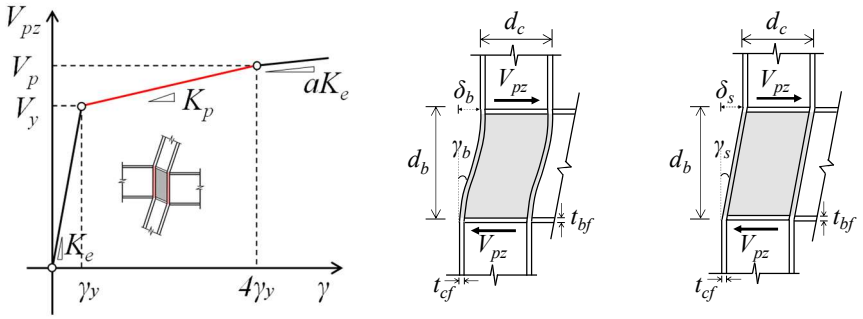

(a) (b) (c)

Fig. 1 – Panel zone mathematical model assumptions and kinematics

$$K_e = \frac{V_y}{\gamma_y} = 0.95 \cdot d_c \cdot t_{cw} \cdot G \tag{1}$$

$$V_y = \frac{f_y}{\sqrt{3}} \cdot 0.95 d_c \cdot t_{cw} \tag{2}$$

$$V_p = \mathrm{V_y} \cdot \left(1 + 3K_p/K_e\right) \tag{3}$$

Where, G is the steel material modulus of rigidity; f_y is the steel material yield stress; t_{cw} is the column web thickness; d_c is the column depth; K_p is the panel zone post-yield stiffness (see Fig. 1a).

Limitations to the aforementioned panel zone model pertain (a) cases involving non-uniform shear stresses in the web at the onset of yielding [12]; (b) cases where the bending deformation is considerable (see Fig. 1b) in addition to the shear deformation [11] (see Fig. 1c). Figure 2a compares the analytically calculated elastic stiffness, K_e, based on Eq. (1) with the measured one, $K_{e,m}$, from collected test data (see http://resslabtools.epfl.ch/). The elastic stiffness K_e is overestimated by 20% because the bending deformation is neglected. A number of researchers [7], [13] adopted a modified panel zone yield shear strength, V_y, and elastic stiffness, K_e, formulation based on limited experimental data.

Regarding the second branch (see Fig. 1a), it is assumed that the panel zone web cannot provide additional shear resistance beyond γ_y. The additional post-yield shear resistance, in this case, is attributed to the surrounding elements. In prior studies, the post-yield stiffness, K_p, was deduced by small-scale subassembly tests with column flange thicknesses t_{cf} ranging from 10mm to 24mm. Studies [11], [13]–[19]

have pointed out that the assumed K_p value does not lead to accurate predictions for columns featuring thick column flanges. The current design practice assumes that the panel zone strength is either equal to V_y [20], [21] or V_p [22]–[24]. In Europe, an additional panel zone shear strength term is accounted for in the presence of continuity plates.

Figure 2b shows the ratio of the predicted over the measured panel zone post-yield strength ratio, $V_p/V_{p,m}$ with respect to t_{cf} based on beam-to-column connection tests that are mostly collected from the SAC program [25]. The straight lines denote the respective trend of the above ratio with respect to t_{cf}. It is observed that the AIJ model [21] consistently underestimates V_p by almost 15%, because the contribution of the column flange is disregarded. The AISC model [23] overestimates V_p by 20-40% for thick column flanges (t_{cf} larger than 50mm). Interestingly, the CEN model [20] exhibits an opposite trend than that of the AISC model. The reason is that the column flange contribution is neglected when continuity plates are not present. This is common in shallow and stocky columns (i.e., heavy W14 in North America or HHD profiles in Europe). However, the expected column flange contribution is substantial in this case. Thus, the panel zone shear strength is underestimated by 20% when t_{cf} is larger than 50mm.

Within such a context, this paper proposes an improved mechanics-based panel zone model for the seismic design of steel MRFs. The model is informed by continuum finite element (CFE) analyses to comprehend the mechanics of the panel zone when it experiences inelastic deformations. The proposed model is validated based on representative panel zone test data available in the literature.

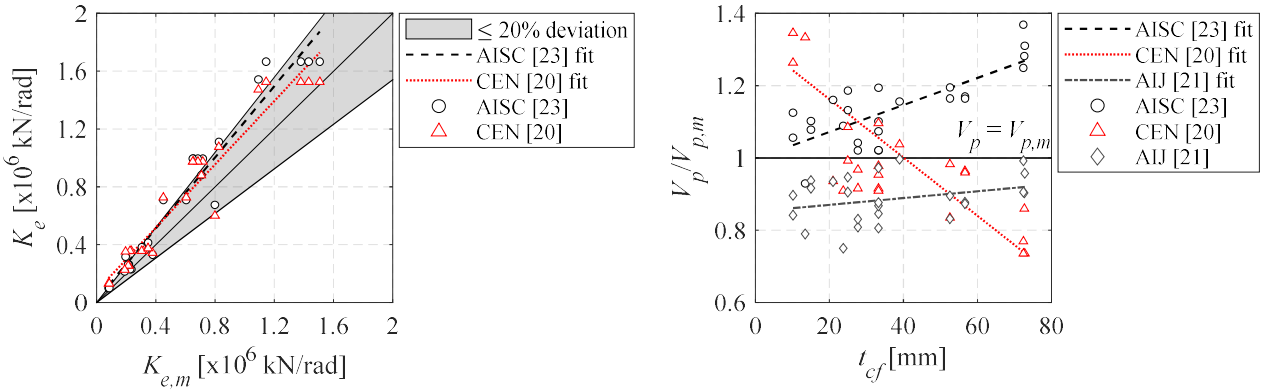

(a) elastic stiffness, K_e (b) post-yield strength, V_p

Fig. 2 – Comparison of analytical and measured panel zone model parameters

2. Finite Element Modeling Details

The commercial finite element analysis software ABAQUS (version 6.14-1) [26] is used to develop the CFE model. The CFE modeling approach, presented herein, is validated with a full-scale beam-to-column connection test (specimen identification: UT04) from a prior experimental program [9]. This connection features a stocky column cross-section (W14x398) along with deep and slender beams (W36x150) made of A992 Gr. 50 steel (nominal yield stress, f_y = 345MPa). All the respective profiles are highly ductile according to the AISC seismic provisions [24].

The utilized multiaxial plasticity material model employs a combined multiaxial isotropic/kinematic hardening law [27]. The input model parameters are identified according to the optimization approach proposed by de Castro e Sousa and Lignos [28]. Local imperfections in the beams are incorporated as discussed in Elkady and Lignos [29]. Residual stresses according to Young [30] are considered as suggested by complementary studies according to de Castro e Sousa and Lignos [31]. In the CFE analyses, twenty-node quadratic brick elements with reduced integration (C3D20R) are employed. The number of elements through thickness are summarized in Fig. 3a for the critical regions within the column and beams, where inelastic

deformations are likely to occur. Outside those regions, a coarser mesh is employed to expedite the CFE analyses. The model boundary conditions and lateral restraints represent those of the physical test (see Fig. 3a). To expedite the analyses, a panel zone web-only CFE model (termed reduced-order hereinafter) is examined as shown in Fig. 3b. Referring to Fig. 3c, the reduced-order model is able to reproduce the panel zone behavior corresponding to the detailed model, which was described earlier, up to $6\gamma_y$. Interestingly, cyclic hardening up to this level of distortion is not appreciable; hence the shear strength of the two models does not deviate from each other by more than 5%. Consequently, the reduced-order CFE model is employed in the subsequent analyses to expedite the computations.

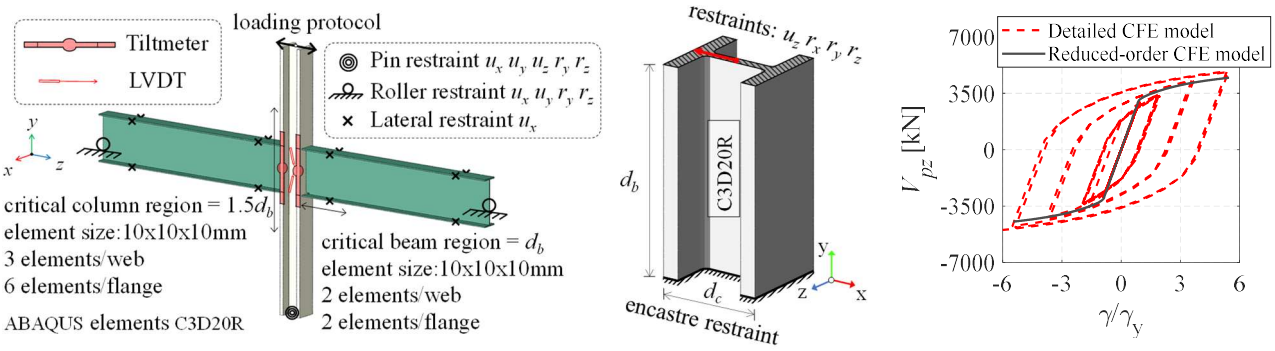

Fig. 3 – Detailed and reduced-order continuum finite element models

Figure 4 shows a comparison of the test data and the CFE analysis results in terms of the global response (applied force, F versus story drift ratio, θ) as well as the individual beam and panel zone contributions to θ. In the test, the panel zone response was obtained from linear variable differential transformers (LVDTs) (see Fig. 3a), while the beam response was deduced from a combination of LVDTs and tiltmeters that were placed in the column flanges as shown in Fig. 3a. The equivalent decomposition approach is followed in the CFE analyses. The agreement between the test and the CFE model results in terms of strength and stiffness is noteworthy and the modeling assumptions are, thus, validated.

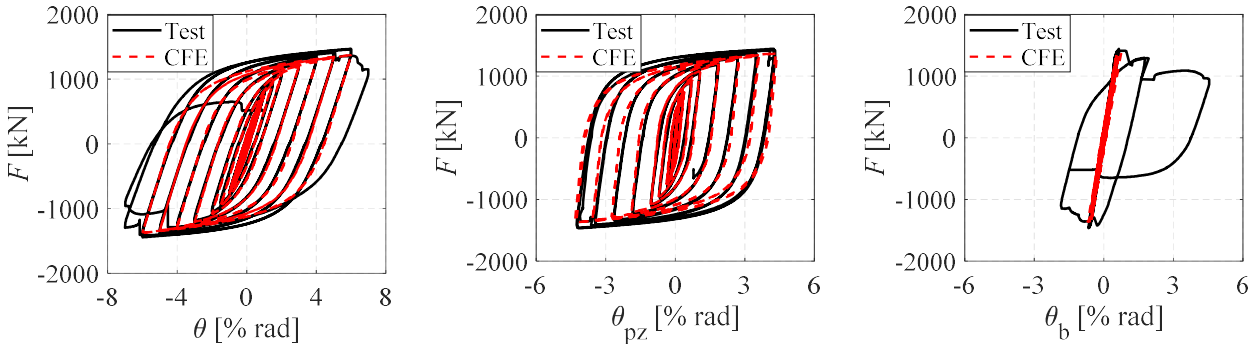

Fig. 4 – Comparison between CFE model predictions and physical test data: data reproduced from Shin [9]

3. Parametric Analyses

We examine eight panel zone geometries to investigate the bending deformation mode effect on the panel zone stiffness and the influence of the column flange thickness on the panel zone shear resistance. The varied parameters are the panel zone aspect ratio, d_b/d_c, the column flange width, b_{cf}, and the column flange thickness, t_{cf}. Monotonic loading is imposed in all cases up to $6\gamma_y$. The deduced parameters from these

analyses are; (a) K_e, defined by the elastic stiffness (in terms of $V_{pz} - \gamma$ relation); (b) V_y, defined based on the yield initiation in the centre of the panel zone; and (c) the post-yield panel zone strength at $4\gamma_y$ and $6\gamma_y$.

Figure 5 depicts representative analyses results for a slender (d_b/d_c = 1.5 and t_{cf} = 25mm) and a stocky (d_b/d_c = 1.0 and t_{cf} = 50mm) panel zone geometry. In the same figure we have superimposed the respective predictions according to the Krawinkler model. In the former case, K_e is about 30% lower than the predicted value, while in the latter both the predicted and measured K_e values agree well. This implies that the effect of the bending deformation mode (see Fig. 1b) is pertinent in slender panel zones while the shear deformation mode (see Fig. 1c) is dominant in stocky ones. Moreover, the elastic stiffness is underestimated by 10% in stocky panel zones. This discrepancy is attributed to the inaccuracy of the assumed panel zone shear area for these geometries [32].

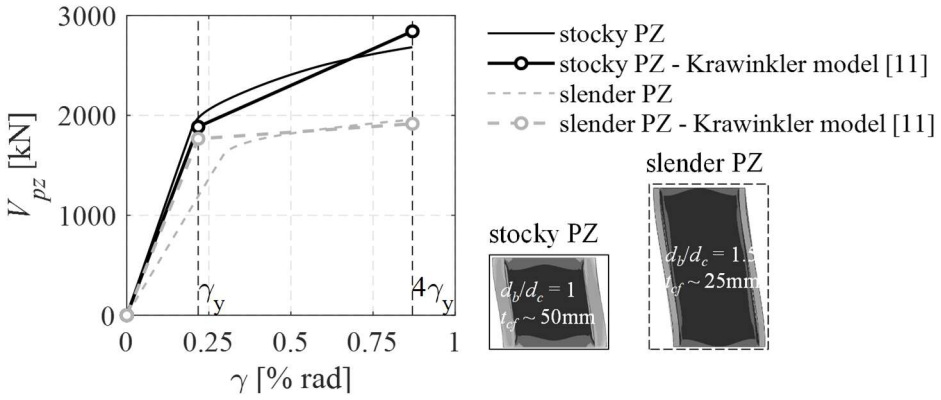

Fig. 5 – Representative CFE analyses results for varying web panel zone aspect ratio and column flange thickness

In slender panel zone geometries, V_y is overpredicted by 10% by the Krawinkler model, whereas in stocky ones, V_y is underpredicted by 10%. In the former case, the Krawinkler model predicts V_p relatively well. However, for columns featuring thick column flanges ($t_{cf} \geq$ 50mm), K_p and V_p are overpredicted by more than 20%. These discrepancies are justified based on the stress distributions within the panel web and column flanges.

Figures 6a and 6b show the shear stress distributions at the mid-height location in the slender and stocky panel zones, respectively. The shear values are normalized by the yield shear stress, τ_y ($\tau_y = f_y/\sqrt{3}$). The shear distortion angles depicted in these figures are γ_y and $4\gamma_y$. Planes that represent the average shear stresses in the web ($\tau_{w,eff}$) and the flanges are also superimposed. In the slender panel zone, the assumption of uniform shear distribution in the web panel is not rational, particularly prior to yielding. On the other hand, in the stocky panel zone, the same assumption is fairly accurate, whereas the column flange shear stresses are not negligible. These stresses range from 0.04-0.2τ_y (depending on the shear distortion angle); hence they may increase the panel zone shear resistance by more than 20%.

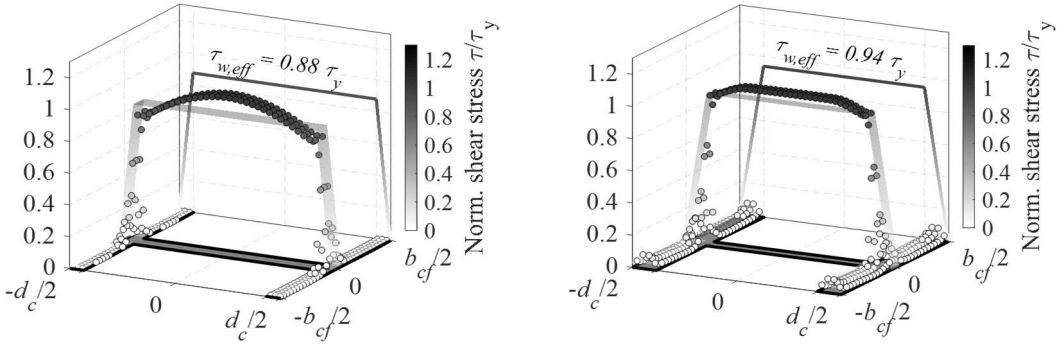

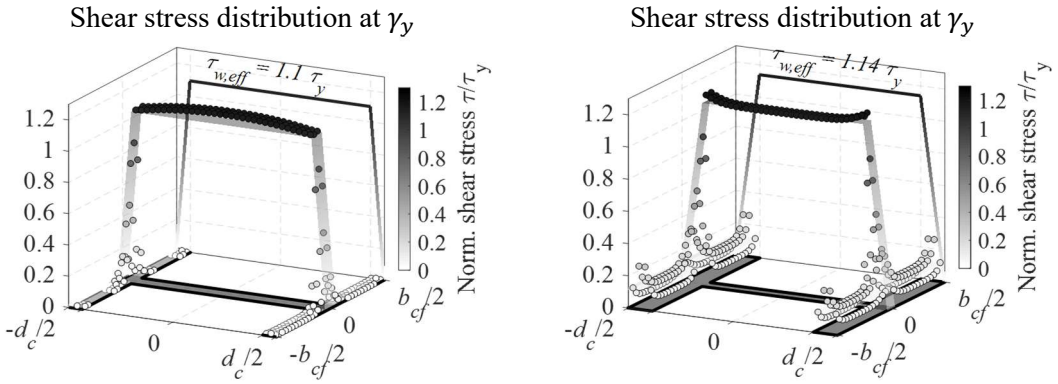

(a) slender panel zone (i.e., d_b/d_c = 1.5 and t_{cf} = 25mm)

(b) stocky panel zone (i.e., d_b/d_c = 1.0 and t_{cf} = 50mm)

Fig. 6 – Shear stress distributions at γ_y and $4\gamma_y$ for various panel zone geometries

4. Proposed Panel Zone Model

4.1 Panel zone elastic stiffness

In the proposed panel zone model, we consider both the shear and bending deformation modes, as shown in Figs. 1b and 1c and expressed in Eq. (4). With regard to the shear stiffness, K_s, the effective shear area, A_v, is based on recommendations by Charney et al. [32] according to Eq. (5). A uniform shear stress in the web and a linear distribution up to zero stress in the outer flange fibre is deemed to be reasonable. As such, the effective panel zone depth can be taken as $d_{eff} = d_c - t_{cf}$. Other models (e.g., AISC model) that assume $d_{eff} = d_c$, overpredict K_e by almost 10% for column cross-sections with t_{cf} larger than 40mm. According to Eq. (6), the panel zone bending stiffness, K_b, assumes a member in contraflexure oriented in its strong axis. Doubler plates would affect both K_s and K_b. As such, we propose that the panel zone thickness be taken as $t_{pz} = t_{cw} + t_{dp}$ [t_{dp} is the total doubler plate(s) thickness]. Moreover, the total doubler plate(s) thickness should be considered in the calculation of the column's strong-axis second moment of area, I,

$$K_e = \frac{V_{pz}}{\gamma} = \frac{K_s \cdot K_b}{K_s + K_b} \tag{4}$$

$$K_s = A_v \cdot G = t_{pz} \cdot (d_c - t_{cf}) \cdot G \tag{5}$$

$$K_b = \frac{12 \cdot E \cdot I}{d_b^3} \cdot d_b \tag{6}$$

where, E is the Young modulus.

4.2 Panel zone shear strength

The column flange contribution, V_f, to the overall panel zone shear resistance, is estimated according to Eq. (7). In this equation, the column flange stiffness with respect to the loading direction, K_f, is computed according to Eq. (8), in which both shear and bending deformation modes are considered. The former mode, K_{sf} [see Eq. (9)], assumes uniform shear stresses in the column flanges, while the latter, K_{bf} [see Eq. (10)], assumes that the column flanges are in contraflexure with respect to their weak axis.

$$V_f = (K_f/K_e) \cdot V_{pz} \tag{7}$$

$$K_f = \frac{K_{sf} \cdot K_{bf}}{K_{sf} + K_{bf}} \tag{8}$$

$$K_{sf} = 2 \cdot (t_{cf} \cdot b_{cf} \cdot G) \tag{9}$$

$$K_{bf} = 2 \cdot \left[\frac{12E(b_{cf} \cdot t_{cf}^3/12)}{d_b^3} \cdot d_b \right] \tag{10}$$

Figure 7 depicts the proposed K_e and V_p, which is discussed later on in this section, deviation from those of the CFE analyses results (noted as "m") with respect to K_f/K_e. The proposed panel zone model parameters are compared with those predicted by the Krawinkler model. Interestingly, for slender panel zone geometries with K_f/K_e < 0.03, where bending deformation is dominant, the proposed model provides an improved estimate of K_e. For stocky panel zones, the proposed model achieves a similar accuracy with the Krawinkler model. Referring to Fig. 7b, the proposed model predicts V_p with remarkable accuracy compared to the Krawinkler model.

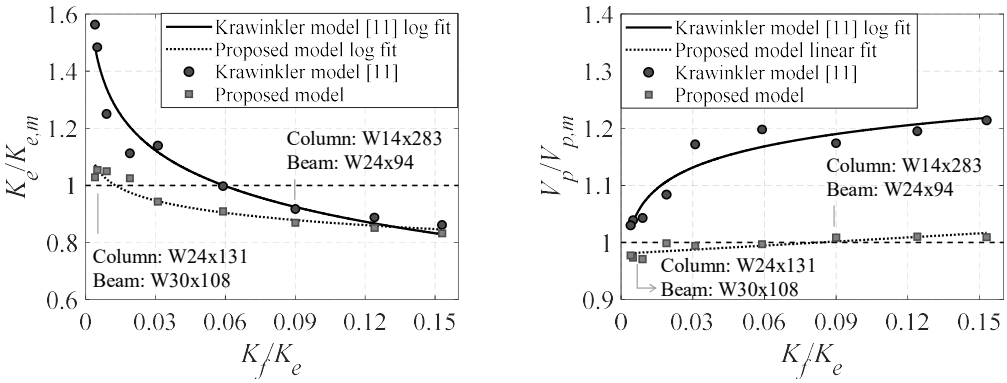

(a) elastic stiffness, K_e (b) post-yield strength, V_p

Fig. 7 – Deviation of predicted panel zone response parameters from measured ones with respect to K_f/K_e

The panel zone shear resistance may be calculated by integrating the shear stresses developed at a plane perpendicular to the column's longitudinal vector, as expressed by Eq. (11). In the calculations presented herein, the panel zone shear strength is taken from the panel zone mid-height plane since the distributed shear demand is maximized at this plane. Double integration is replaced by double summation in the discrete finite elements as given by Eq. (12). In this equation, the parameters a_w and a_f represent the normalized shear stresses (normalized with respect to the yield shear stress, τ_y) at any flange and web finite element in the panel zone plane.

$$V_{pz} = \iint_A \tau dA = \iint_{A_w} \tau dA_w + 2 \iint_{A_f} \tau dA_f \tag{11}$$

$$V_{pz} = \frac{f_y}{\sqrt{3}} \cdot \sum_{-d_c/2}^{d_c/2} \sum_{-t_{cw}/2}^{t_{cw}/2} a_w(x,y)\delta x \delta y + \frac{f_y}{\sqrt{3}} \cdot 2 \sum_{-b_{cf}/2}^{b_{cf}/2} \sum_{-t_{cf}/2}^{t_{cf}/2} a_f(x,y)\delta x \delta y \tag{12}$$

Where, A is the column cross section area at the plane of interest; A_w is the column web area; A_f is the area of each column flange.

The panel zone shear strength calculation based on Eq. (12) requires the shear stress distribution at the shear distortion level of interest. In an effort to simplify the expression, the average web and flange shear stresses are introduced in Eq. (13) to calculate the panel zone shear resistance. Therefore, the a_w and a_f

parameters are replaced by the normalized average shear stresses in the web and the flange (i.e., $a_{w,eff}$ and $a_{f,eff}$, respectively).

$$V_{pz} = a_{w,eff} \cdot \frac{f_y}{\sqrt{3}} \cdot (d_c - t_{cf}) \cdot t_{cw} + a_{f,eff} \cdot \frac{f_y}{\sqrt{3}} \cdot (b_{cf} - t_{cw}) \cdot 2t_{cf}$$
$$a_{w,eff} = \frac{\sum_{-d_c/2}^{d_c/2} \sum_{-t_{cw}/2}^{t_{cw}/2} \tau_w \delta x \delta y}{t_{cw} \cdot (d_c - t_{cf}) \cdot \tau_y}, \text{ and } a_{f,eff} = \frac{\sum_{-b_{cf}/2}^{b_{cf}/2} \sum_{-t_{cf}/2}^{t_{cf}/2} \tau_f \delta x \delta y}{t_{cf} \cdot b_{cf} \cdot \tau_y} \quad (13)$$

Figure 8 depicts the relationship of $a_{w,eff}$ and $a_{f,eff}$ with respect to K_f/K_e at three different distortion levels pertinent to seismic design. The high coefficient of determination (i.e., $R^2 > 0.95$) of these relationships demonstrates the efficiency and sufficiency of K_f/K_e to describe the shear stress evolution within the panel zone joint.

Referring to Fig. 8a, for high shear distortion angles ($> 4\gamma_y$), the average web shear stresses attain $1.2\tau_y$. The shear stress distribution in the web does not depend on the panel zone geometry for distortion angles larger than $4\gamma_y$. Referring to Fig. 8b, the average shear stresses in the column flanges appear substantially lower than those in the column web. This is more evident for slender panel zones ($K_f/K_e < 0.02$). However, for distortion angles larger than $4\gamma_y$, in stocky panel zones ($K_f/K_e > 0.06$), the column flange contribution to the panel zone shear resistance can be more than 20%.

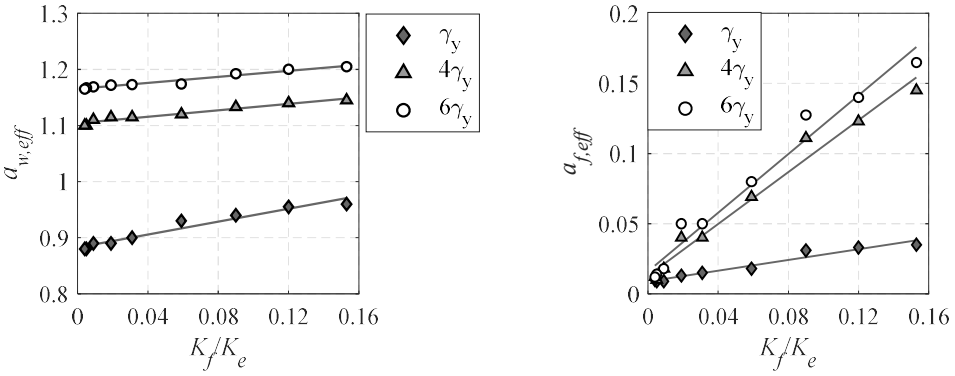

(a) web (b) flange

Fig. 8 – Normalized average shear stresses at γ_y, $4\gamma_y$ and $6\gamma_y$

Although the average shear stress parameters may be effectively related to K_f/K_e, simplified equations are provided herein that could be directly used in prospective seismic design provisions of steel MRFs. Since the column flange contribution to the panel zone shear strength at γ_y is negligible, regardless of the panel zone geometry, V_y is expressed based on the web shear resistance. This assumption is consistent with the current practice. However, two panel zone geometry groups are adopted; (a) slender panel zones with $K_f/K_e < 0.02$ and (b) stocky panel zones with $K_f/K_e > 0.06$. The proposed V_y is given by Eq. (14) for the adopted panel zone geometries. In all other cases, interpolation is proposed. For higher panel zone distortion angles (i.e., $4\gamma_y$ and $6\gamma_y$) pertinent to seismic design, $a_{w,eff}$ may be kept constant regardless of the K_f/K_e, whereas, $a_{f,eff}$ depends on the panel zone geometry itself (see Table 1). The proposed panel zone shear strength in this case is given by Eq. (15) based on recommended values that are summarized in Table 1.

$$V_y = \frac{f_y}{\sqrt{3}} \cdot a_y \cdot (d_c - t_{cf}) \cdot t_{cw}, \text{ where } a_y = 0.9 \text{ and } 1.0 \text{ for slender and stocky panel zone geometries, respectively} \quad (14)$$

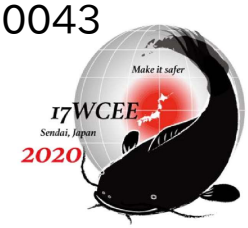

$$V_{pz} = \frac{f_y}{\sqrt{3}} \cdot \left[a_{w,eff} \cdot (d_c - t_{cf}) \cdot t_{cw} + a_{f,eff} \cdot (b_{cf} - t_{cw}) \cdot 2t_{cf} \right] \quad (15)$$

Table 1 – Panel zone model normalized average shear stress parameters for the web and the flanges at $4\gamma_y$ and $6\gamma_y$

Panel zone geometry	Web ($a_{w,eff}$)		Flange ($a_{f,eff}$)	
	$4\gamma_y$ (V_p)	$6\gamma_y$ ($V_{6\gamma y}$)	$4\gamma_y$ (V_p)	$6\gamma_y$ ($V_{6\gamma y}$)
Slender	1.1	1.15	0.02	0.03
Stocky			0.1	

4.3 Model validation with physical test data

The proposed model is validated with available physical test data from the literature [9], [33]. Figure 9 shows a comparison of the predictions, based on the proposed model, and with test data from a slender and a relatively stocky panel zone. The former is specimen A1; tested by Krawinkler et al. [33] and comprises W10x15 beams and a W8x24 column without doubler plates (K_f/K_e = 0.01). The latter is specimen UT05; tested by Shin [9] and features W36x150 beams and a W14x398 column with two doubler plates 13mm thick each (K_f/K_e = 0.05). In the same figure, we have superimposed the AISC model for reference.

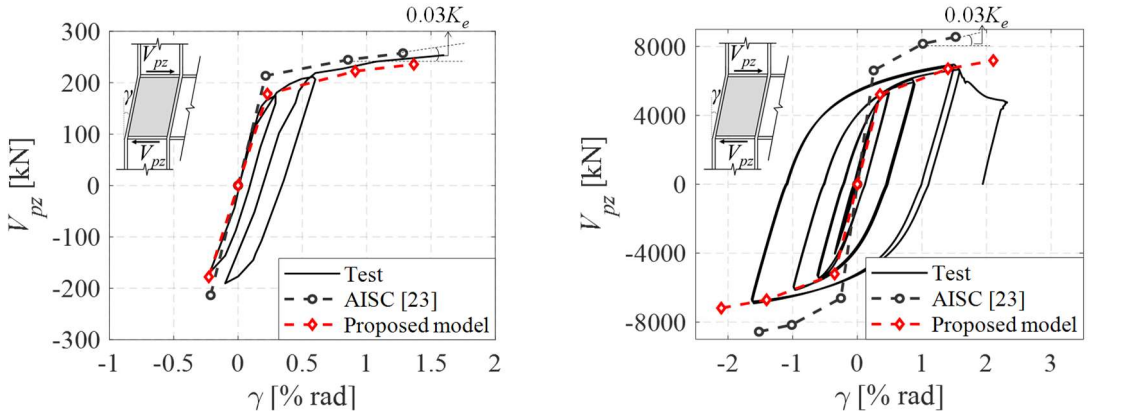

(a) Slender panel zone, K_f/K_e = 0.01 (specimen A1, [33])

(b) Stocky panel zone, K_f/K_e = 0.05 (specimen UT05, [9])

Fig. 9 – Comparison of test and predicted panel zone hysteretic responses

Referring to Fig. 9a, the AISC model overpredicts the measured K_e value by 20% because the model neglects the bending deformations of the panel zone. Similarly, V_y is overestimated by 20% by the AISC model because the assumed uniform web shear yield stress distribution is not rational. From the same figure, the AISC model predicts well V_p. However, specimen A1 [33] had been considered in the derivation of the Krawinkler model.

Referring to Fig. 9b, the AISC model overestimates all the panel zone parameters of interest (i.e., K_e, V_y, V_p) by more than 20%. On the other hand, the proposed model demonstrates superior performance in predicting both the stiffness and shear strength of the panel zone regardless of its geometry.

5. Limitations of the Study

The proposed panel zone model is applicable to wide-flange column cross-sections. We have not conducted validations with columns comprised of hollow structural sections. In this case, a similar methodology to the one presented herein may be followed to extract the corresponding shear stress distributions within the panel

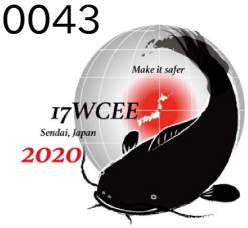

zone. Specific care should be given to the considered residual stresses in this case. The role of the doubler plate to the panel zone shear resistance has not been investigated herein. However, the authors are working towards this objective.

6. Summary and Conclusions

We proposed an improved panel zone model in support of seismic design of steel MRFs. The model is based on realistic web and flange shear stress distributions within a broad range of geometries. For this purpose, continuum finite element (CFE) simplified models were employed. The modeling strategy was thoroughly validated based on a typical post-Northridge interior subassembly physical data. An updated expression of the panel zone stiffness that accounts for both shear and bending deformations is proposed. Improved expressions are also developed to predict the panel zone shear strength at three different distortion angles pertinent to current seismic provisions promoting a balanced panel zone design.

When the bending deformation mode of the panel zone is neglected, its elastic stiffness, K_e, is overestimated by more than 20%, especially for slender panel zone geometries with beam-to-column depth ratios, $d_b/d_c \geq 1.5$. Therefore, the proposed elastic stiffness expression [see Eq. (4)] accounts for both shear and bending panel zone deformation modes. Predictions of the panel zone's elastic stiffness with Eq. (4) depict relatively well measured values from available panel zone physical tests of representative geometries.

The CFE results suggest that the common uniform web shear stress assumption is only valid for stocky panel zones. For slender panel zone geometries, the above assumption tends to overestimate the actual shear strength by more than 10%.

The proposed equation for V_y [see Eq. (14)] achieves a similar accuracy with that of the Krawinkler model or the AISC model for shear deformation-dominant panel zone geometries. However, the proposed equation enjoys a superior accuracy for slender panel zone geometries, where the web shear stress distribution is non-uniform.

While the current AISC model overpredicts V_p by more than 30% in panel zone geometries featuring thick column flanges ($t_{cf} \geq 50$mm), the proposed expression for V_p [see Eq. (15)] provides a remarkable accuracy as demonstrated by direct comparisons with available physical data.

6. Acknowledgements

This study is based on work supported by a Nippon Steel Corporation collaborative grant as well as an EPFL internal grant for the first author. The financial support is gratefully acknowledged. The authors would like to sincerely thank Prof. Bozidar Stojadinovic from ETH-Zürich, for providing test data for the development of the inelastic panel zone database that is used as part of the present study. Any opinions, findings, and conclusions or recommendations expressed in this paper are those of the authors and do not necessarily reflect the views of sponsors.

7. References

[1] Chi WM, Deirlein GG, Ingraffea A (1997): Finite element fracture mechanics investigation of welded beam-column connections. Cornell University, Ithaca, New York, SAC/BD-97/05.

[2] El-Tawil S, Mikesell T, Vidarsson E, Kunnath SK (1998): Strength and ductility of FR welded-bolted connections. Universtiy of Central Florida, Orlando, Florida, SAC/BD-98/01.

[3] Lu LW, Ricles JM, Mao C, Fisher JW (2000): Critical issues in achieving ductile behaviour of welded moment connections. *Journal of Constructional Steel Research*, **55**(1–3), 325–341.

[4] Mao C, Ricles J, Lu LW, Fisher J (2001): Effect of local details on ductility of welded moment connections. *Journal of Structural Engineering*, **127**(9), 1036–1044.

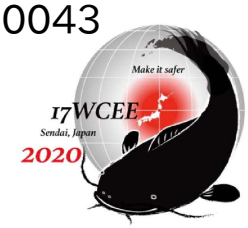

[5] Lee CH, Jeon SW, Kim JH, Uang CM (2005): Effects of panel zone strength and beam web connection method on seismic performance of reduced beam section steel moment connections. *Journal of Structural Engineering*, **131**(12), 1854–1865.

[6] Lee D, Cotton SC, Hajjar J, Dexter RJ, Ye Y (2005): Cyclic behavior of steel moment-resisting connections reinforced by alternative column stiffener details I. connection performance and continuity plate detailing. *Engineering Journal*, **42**, 189–214.

[7] Lin KC, Tsai KC, Kong SL, Hsieh SH (2000): Effects of panel zone deformations on cyclic performance of welded moment connections. *12th WCEE*, Auckland, New Zealand, Paper No. 1252.

[8] Rahiminia F, Namba H (2013): Joint panel in steel moment connections, Part 1: Experimental tests results. *Journal of Constructional Steel Research*, **89**, 272–283.

[9] Shin S (2017): Experimental and analytical investigation of panel zone behavior in steel moment frames. PhD Thesis, University of Texas at Austin.

[10] Tsai KC, Chen WZ (2000): Seismic responses of steel reduced beam section to weak panel zone moment joints. *Behaviour of Steel Structures in Seismic Areas, STESSA 2000*, Montreal, Canada, 279–286.

[11] Krawinkler H (1978): Shear in beam-column joints in seismic design of steel frames. *Engineering Journal*, **15**(3), 82–91.

[12] Tsai KC, Popov EP (1988): Steel beam-column joints in seismic moment resisting frames. University of California, Berkeley, CA.

[13] Kim KD, Engelhardt MD (2002): Monotonic and cyclic loading models for panel zones in steel moment frames. *Journal of Constructional Steel Research*, **58**(5–8), 605–635.

[14] Brandonisio G, De Luca A, Mele E (2012): Shear strength of panel zone in beam-to-column connections. *Journal of Constructional Steel Research*, **71**, 129–142.

[15] El-Tawil S, Vidarsson E, Mikesell T, Kunnath SK (1999): Inelastic behavior and design of steel panel zones. *Journal of Structural Engineering*, **125**(2), 183–193.

[16] Jin J, El-Tawil S (2005): Evaluation of FEMA-350 seismic provisions for steel panel zones. *Journal of Structural Engineering*, **131**(2), 250–258.

[17] Lee D, Cotton SC, Hajjar JF, Dexter RJ, Ye Y (2005): Cyclic behavior of steel moment-resisting connections reinforced by alternative column stiffener details II. panel zone behavior and doubler plate detailing. *Engineering Journal*, **42**(4), 215–238.

[18] Qi L, Paquette J, Eatherton M, Leon R, Bogdan T, Popa N, Nunez E (2018): Analysis of fracture behavior of large steel beam-column connections. *12th International Conference on Advances in Steel-Concrete Composite Structures - ASCCS 2018*.

[19] Soliman AA, Ibrahim OA, Ibrahim AM (2018): Effect of panel zone strength ratio on reduced beam section steel moment frame connections. *Alexandria Engineering Journal*, **57**(4), 3523–3533.

[20] CEN (2005): EN 1993-1-8: Eurocode 3: Design of steel structures – Part 1-8: Design of joints. European Committee for Standardization, Brussels, Belgium.

[21] AIJ (2012): Recommendations for design of connections in steel structures. Architectural Institute of Japan, Tokyo (in Japanese).

[22] CSA (2019): Design of steel structures. Mississauga, Canada: CSA.

[23] AISC (2016): *Specification for structural steel buildings, ANSI/AISC 360-16*. Chicago, IL: American Institute for Steel Construction.

[24] AISC (2016): *Seismic provisions for structural steel buildings, ANSI/AISC 341-16*. Chicago, IL: American Institute for Steel Construction.

[25] Mahin SA (1998): Lessons from damage to steel buildings during the Northridge earthquake. *Engineering Structures*, **20**(4–6), 261–270.

[26] ABAQUS (2014): ABAQUS analysis user's manual version 6.14-1. Dassault Systems Simulia Corp., RI, USA.

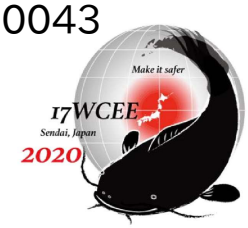

[27] Lemaitre J, Chaboche JL (1990): *Mechanics of solid materials*. Cambridge, UK: Cambridge University Press.

[28] Sousa A, Lignos DG (2018): On the inverse problem of classic nonlinear plasticity models. EPFL, Lausanne.

[29] Elkady A, Lignos DG (2018): Improved seismic design and nonlinear modeling recommendations for wide-flange steel columns. *Journal of Structural Engineering*, **144**(9), 04018162.

[30] Young B (1972): Residual stresses in hot-rolled members. *Paris*, 1–30.

[31] Sousa A, Lignos DG (2017): Residual stress measurements of European hot-rolled I-shaped steel profiles. EPFL, Lausanne.

[32] Charney FA, Iyer H, Spears PW (2005): Computation of major axis shear deformations in wide flange steel girders and columns. *Journal of Constructional Steel Research*, **61**(11), 1525–1558.

[33] Krawinkler H, Bertero VV, Popov EP (1971): Inelastic behavior of steel beam-to-column subassemblages. EERC, University of California, Berkeley.

